Spatiotemporal Vectorial Solitons in Nonlinear Ultrafast Dual-Core Fiber Lasers

Boyao Li,[*,†,‡] Xingjie Wang,[†,‡] Yaoyao Liang,[*,¶] Jinghua Sun,[†,‡] and Guiyao Zhou[‡]

†*School of Electronic Engineering and Intelligentization, Dongguan University of Technology, Dongguan, Guangdong, 523808, China*

‡*Guangzhou Key laboratory for Special Fiber Photonic Devices and Applications, School of Information Optoelectronics Science and Technology, Guangzhou, Guangdong 510006, China*

¶*Centre de Nanosciences et de Nanotechnologies, CNRS, Univ. Paris-Sud, Université Paris-Saclay, C2N – 10 Boulevard Thomas Gobert – 91120 Palaiseau, France*

E-mail: liby@dgut.edu.cn; yaoyao.liang@universite-paris-saclay.fr

Abstract

The processes of soliton generation and interference focus on the complex nonlinear soliton dynamics resembling matter particles. In order to further understand the dynamic process of solitons from a multidimensional perspective, here we report the vectorial solitons nature under two-sets pulse splitting in a single cavity induced by dual-core fiber assisted ultrafast fiber lasers. Owing to the weakly coupled cores in symmetrical dual core fiber (SDCF), two pulse groups interaction are formed in a cavity. By using the dispersive Fourier transformation technique (DFT), it was found that the four-component polarized rotation vector solitons (PRVS) generate. Moreover, gradually increasing the power can obtain the locked soliton bound state in two core space,

 doi:10.20944/preprints202210.0243.v2

and the corresponding evolution is similar to that of non-degenerate bright solitons in Bose Einstein condensates (BEC). In addition, by properly controlling the soliton phase offset in SDCF, the soliton rain state of multi pulse evolution can be obtained. The related experimental results would be fruitful to the communities interested in soliton dynamics and frequency comb lasers.

Key words: BEC; Ultrafast Lasers; Fibers

Introduction

As an ideal light source for generating high-performance ultra-short pulses, ultrafast fiber lasers have been extensively studied for both providing the widespread applications in ultrafast spectroscopy, frequency comb, micromachining, biomedical imaging and serving as an experimental platform towards the exploration of nonlinear dynamics.[1–3] Meanwhile, mode locking technology is an important technology to generate ultrashort pulses, which determines the characteristics of ultrashort pulses. For furtherly studying the characteristics of ultrashort pulses, the main mode locking technologies developed so far include active mode locking and passive mode locking. Compared to active mode-locking techniques, passive mode-locking techniques possess the advantages of compactness, flexibility and improved performance.[4] Therefore, various passive mode-locking techniques have been employed in ultrafast fiber lasers, such as nonlinear amplified loop mirror (NALM),[5] nonlinear optical loop mirror,[6] nonlinear polarization rotation (NPR),[7] semiconductor saturable absorber mirror,[8] carbon nanotube,[9] graphene and transition metal dichalcogenides.[10]

In addition, mode locking is due to the introduction of a fixed phase relationship between different modes in the laser resonator, and the interference between modes will produce a series of pulses. When the laser cavity parameters remain unchanged, once multiple soliton pulses are generated, these pulses will exist stably in the cavity and will not disappear or generate new pulses with the passage of time.[11] These soliton pulses can act directly or indirectly through dispersive wave, continuous wave and other interference effects, which will lead to the generation of multi soliton pulses with different shapes, including bound

 doi:10.20944/preprints202210.0243.v2

solitons,[12] harmonic pulses,[13] bound soliton strings,[14] soliton rain and so on.[15,16] It can be seen not only mode-locked solitons are inseparable from the interference effect, but also the generation of multi soliton pulses. Thus, the study of the interference between solitons in fiber lasers is of great significance to the study of soliton dynamics. The common interference effects in fiber lasers include polarization interference,[17] nonlinear mode interference,[18] Mach Zehnder interference,[19] etc. Through different interference mechanisms, a wealth of soliton interaction phenomena can be observed, which deepen our understanding of the nonlinear dynamic characteristics of soliton evolution.

However, limited by one dimensional waveguide modes characteristics in the cavity, the formal basis of soliton interaction is based on one-channel fundamental mode. To realize mode locking dynamics akin to the pulse effect of modes division multiplexing, Wright et al. proposed a locking-mode mechanism in multimode fiber, which allows locking of multiple transverse and longitudinal modes to create ultrashort pulses with a variety of spatiotemporal profiles.[20] Nevertheless, due to the single-core character of the fiber, these soliton pulses interferences are interactions among single-dimensional solitons, which are of some difficulties and inconveniences in practical to manipulate the solitons independently at will. In contrast, transverse multi-dimensional soliton interactions have more degrees of freedom, which can deepen the understanding of soliton interaction.

Therefore, for further studying the interaction between multi-dimensional solitons, a symmetrical dual core fiber (SDCF) is proposed as multi-dimensional soliton interference path in this paper. Because the two weakly coupled cores in SDCF are far away, which makes the single soliton pulse or pulse group become a two-way soliton pulse group for interference and evolution in the laser cavity. In order to better study the complex dynamic process between the polarization components of the vector characteristics, the time stretch dispersive Fourier transform technology (DFT)[21] is used to capture real-time spectral information for recording the dynamic events in the time domain and spectral domain in the form of snapshots. The evolution results of DFT show the four-component polarized rotation vector solitons (PRVS)

Preprints (www.preprints.org) | NOT PEER-REVIEWED | Posted: 24 October 2022 doi:10.20944/preprints202210.0243.v2

generates in the cavity because two sets of mode-locked optical paths in the dual core coexist in one cavity. Furthermore, the generation of soliton bound states is realized by increasing the pump power and nonlinearity. Compared with degenerate bright solitons in Bose Einstein condensates (BEC), the results indicate that the laser cavity assisted by SDCF can be used as the analysis platform of soliton phenomenon in two-component BEC. Besides, the evolution of multi pulse soliton rain in the above bound state can be formed by adding a certain bias phase to the pulse in the cavity. These results unveil the transient dynamics with more degrees of freedom as well as highlight the possible application for optical frequency comb, multi pules space division multiplexing and verification physical phenomena of BEC.

Experimental setup

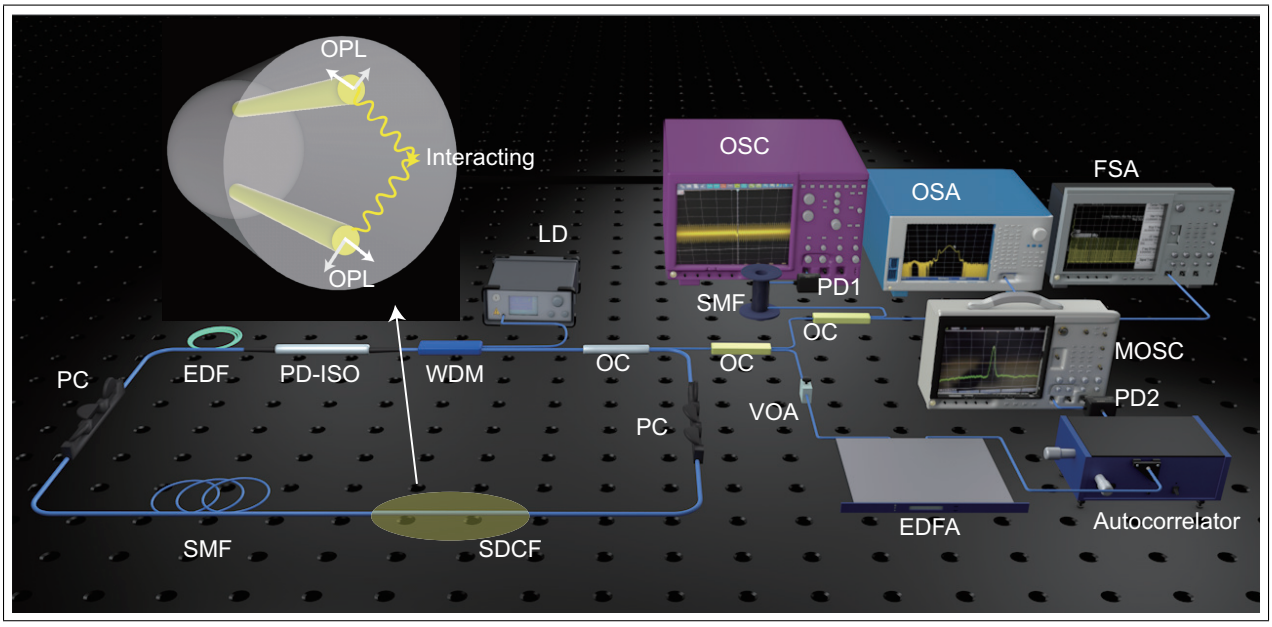

Figure 1: Schematic illustration of the fiber laser cavity and measurement setup.

The schematic of the SDCF assisted fiber laser and DFT-based real-time spectral measurement system are shown in Fig. 1. As the gain medium, a piece of ∼2.4 m EDF (er110-4/125um, $\beta_2 = 0.051ps^2$) is pumped by a 980 nm laser diode through a 980/1550 nm wavelength-division multiplexer (WDM) /isolator hybrid module. This module also en-

 doi:10.20944/preprints202210.0243.v2

sures the unidirectional oscillation of the fiber laser. In laser cavity, a segment of ∼0.01m SDCF provides two channels for orthogonally polarized light (OPL, i.e., x-polarized light and y-polarized light), and forms the two parts interaction of transverse multiple solitons. The unidirectional operation is ensured by a polarization-dependent isolator (PD-ISO). In addition, a fiber-based polarizer sandwiched by two polarization controllers (PCs) is introduced to initialize the nonlinear polarization rotation (NPR)-based mode-locking. The other fibers in the laser cavity are ∼12.6 m single-mode fiber. Thus, the whole cavity length is about ∼15 m. In the experiment, an 80:20 optical coupler (OC) is externally connected with a 50:50 OC. The branch of one optical path is used to simultaneously measure time domain and spectrum information of ultrashort pulse by an optical spectrum analyzer (OSA, Agilent 86142B) and a high-speed real-time oscilloscope (OSC, Tektronix DSA-70804, 8 GHz) with a photodetector (PD1, Newport 818-BB-35F, 12.5 GHz). Besides, DFT (composed of a 15km single-mode fiber and high-speed real-time oscilloscope) can also be added to this branch to stretch the dispersion of output soliton pulse and observe the real-time evolution of the spectrum in the time domain. Besides, the other branch is connected with autocorrelation for measuring soliton pulse state. Considering the low power of one optical path separated by the beam splitter, an erbium-doped fiber amplifier (EDFA, ltran-1550-edfa) is added in front of the autocorrelator to amplify the optical power of the signal light, in this case the normal measurement conditions of the autocorrelator can be satisfied. At the same time, in order to prevent the high output power after amplification from affecting the measurement of pulse state, a power attenuator (VOA) needs to be added before EDFA to regulate the output power. Finally, the optical path is connected with a micro-oscilloscope (MOSC) through a high-speed photodetector (PD2, HP 11982a) to analyze the autocorrelation curve, and the frequency information output by the laser is measured by a frequency spectrum analyzer (FSA, Agilent E447A).

Preprints (www.preprints.org) | NOT PEER-REVIEWED | Posted: 24 October 2022 doi:10.20944/preprints202210.0243.v2

Results and discussion

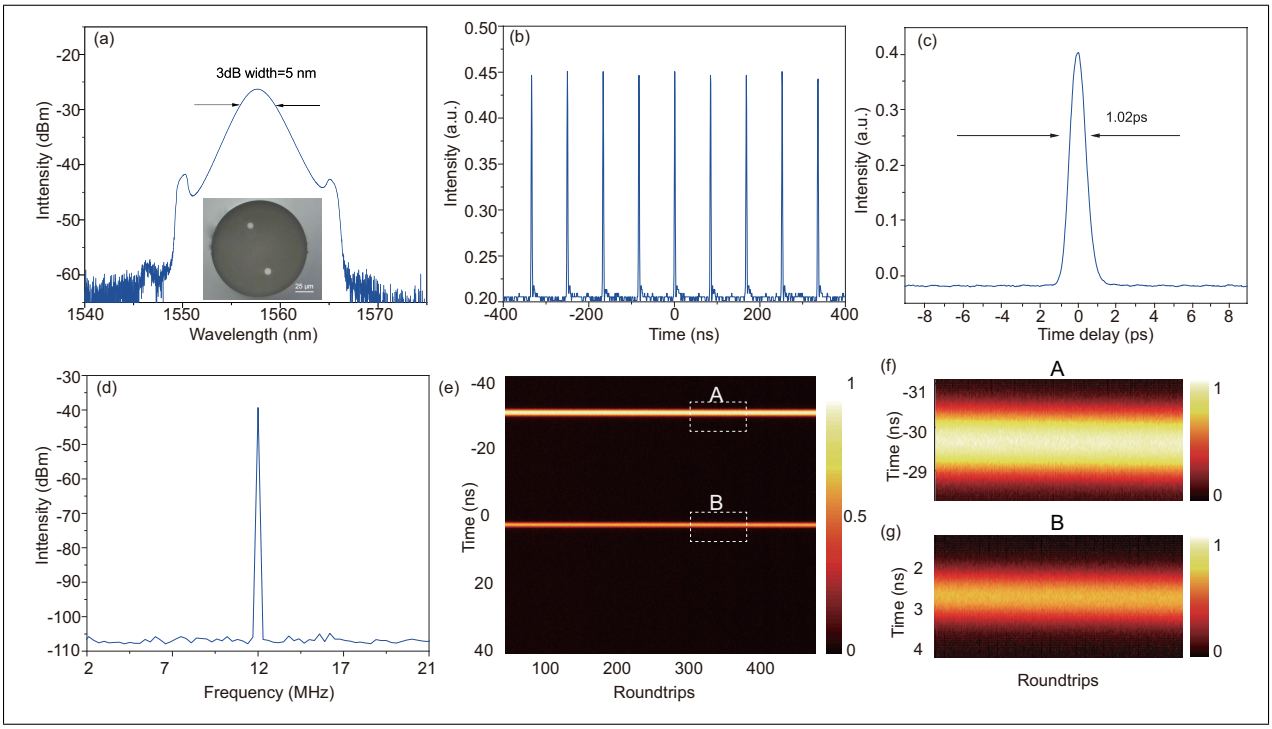

Figure 2: Group velocity locked vector solitons. (a) Optical spectrum, inset is the cross-section image of fabricated dual core fiber; (b) temporal pulse trains based on the oscilloscope; (c) the autocorrelation evolution trac; (d) Rf spectrum; (e) Results of DFT; The zoom-in images of region A and B in (e) are shown in (f) and (g), respectively.

The self-starting locking mode operation of the laser can be realized by reasonably adjusting the state of the intracavity polarization controller and increasing the pump power to exceed the mode locking threshold of the laser (about 250 mW). Continue to increase the pump power to 490mw, and the laser is in a stable mode-locked operation state. At this time, the output power is 170 μw. Due to the dual core characteristic of SDCF, the transmitted pulse automatically evolves into vector solitons. Fig. 2 (a) shows the spectrum of group velocity locked vector solitons (GVLVS). The central wavelength is about 1558nm and the 3dB bandwidth is about 5 nm. The obvious Kelly sideband can be observed from the spectrum, which demonstrates that the laser works in the net negative dispersion region, and the output pulse is a traditional soliton pulse.[22] Fig. 2(b) shows the time pulse sequence. By calculating the adjacent pulse interval, it can be seen that the repetition frequency is

Preprints (www.preprints.org) | NOT PEER-REVIEWED | Posted: 24 October 2022 doi:10.20944/preprints202210.0243.v2

12 MHz, which corresponds to the fundamental frequency determined by the total cavity length of 15m. Fig. 2 (c) shows the autocorrelation curve, and the pulse duration is 1.02ps. The RF spectrum in Fig. 2 (d) shows a repetition rate of 12 MHz and a signal-to-noise ratio (SNR) of more than 60dB, which is agree with Fig. 2(b). In order to further study the evolution of intracavity pulse in SDCF, we recorded the pulse trains before and after the DFT by an oscilloscope as shown in Fig. 2(e). It can be seen two pulses separated in time generate in the laser cavity, which indicates SDCF divides the pulse into two parts in the transverse space in the cavity. Then two sets of group velocity vector locking pulses are formed. The main reason for the formation of GVLVS in the cavity is that the two cores of SDCF become independent channels for two orthogonal polarization components transmitting due to the weak coupling property. At this time, there are two sets of orthogonal polarization soliton components in the SDCF, that is, four polarization components will interfere in the single-mode fiber. Considering obvious polarization sensitivity in nonlinear polarization rotation mode locking, by adjusting the PC, the polarization components of two sets of vector solitons are coupled into a non-dispersive unit under the action of cross phase modulation, which transmits in the cavity at the same group velocity. Then, the group velocity difference caused by the difference of the central wavelength of the soliton in the orthogonal polarization direction can compensate that caused by net birefringence.

Since the two-pulse components are in the same cavity, the repetition frequency and evolution of the pulse remain consistent due to the frequency traction of the cavity. In fact, the two sets of pulses in two cores can be regarded as two components, and the solitons of the corresponding components can be regarded as quasi particles. Based on this, under the mean field theory, the two-component quasi one-dimensional BEC of attractive interaction can be described by the following dimensionless 1+1-dimensional two-component nonlinear Schrodinger equation[23,24]

$$i\Psi_{1,t} + \Psi_{1,xx} + 2\left(|\Psi_1|^2 + |\Psi_2|^2\right)\Psi_1 = 0 \tag{1}$$

Preprints (www.preprints.org) | NOT PEER-REVIEWED | Posted: 24 October 2022 doi:10.20944/preprints202210.0243.v2

$$i\Psi_{2,t} + \Psi_{2,xx} + 2\left(|\Psi_1|^2 + |\Psi_2|^2\right)\Psi_2 = 0 \tag{2}$$

Wherein, $\Psi_1(x,t)$ and $\Psi_2(x,t)$ are the condensed body wave functions of the two components respectively. Considering that the dual core fiber is a weakly coupled fiber, the corresponding soliton effect in BEC can be non-degenerate bright soliton. Then, a nondegenerate bright soliton solution is constructed. The lax equation[24] of the model (1) is

$$\begin{aligned} \Omega_x &= U\Omega \\ \Omega_t &= V\Omega \end{aligned} \tag{3}$$

In Eq. (2), U and V are the corresponding intrinsic potential fields, which can be described as following:

$$\begin{aligned} U &= \begin{bmatrix} -i\frac{2}{3}\omega_j & \Psi_1 & \Psi_2 \\ -\Psi_1^* & i\frac{1}{3}\omega_j & 0 \\ -\Psi_2^* & 0 & i\frac{1}{3}\omega_j \end{bmatrix} \\ V &= U\omega_j + \begin{bmatrix} i|\Psi_1|^2 + i|\Psi_2|^2 & i\Psi_{1x} & i\Psi_{2x} \\ -i\Psi_{1x}^* & -i|\Psi_1|^2 & -i\Psi_2\Psi_1^* \\ -i\Psi_{2x}^* & -i\Psi_2^*\Psi_1 & -i|\Psi_2|^2 \end{bmatrix} \end{aligned} \tag{4}$$

The symbol "*" indicates complex conjugation. Based on the zero seed solution $\Psi_1(0) = 0$, $\Psi_2(0) = 0$, it is easy to obtain the special solution of the lax equation Ω_j , which is

$$\Omega_j = \begin{bmatrix} \Omega_{1j} \\ \Omega_{2j} \\ \Omega_{3j} \end{bmatrix} = \begin{bmatrix} e^{-2\tau_j} \\ \beta_j e^{\tau_j} \\ \gamma_j e^{\tau_j} \end{bmatrix}, \tau_j = \frac{i}{3}\omega_j x + \frac{i}{3}\omega_j^2 t \tag{5}$$

The parameters β_j and γ_j are the coefficients of the special solution, and they can take any complex number. In order to construct nondegenerate bright soliton solutions, the special

Preprints (www.preprints.org) | NOT PEER-REVIEWED | Posted: 24 October 2022 doi:10.20944/preprints202210.0243.v2

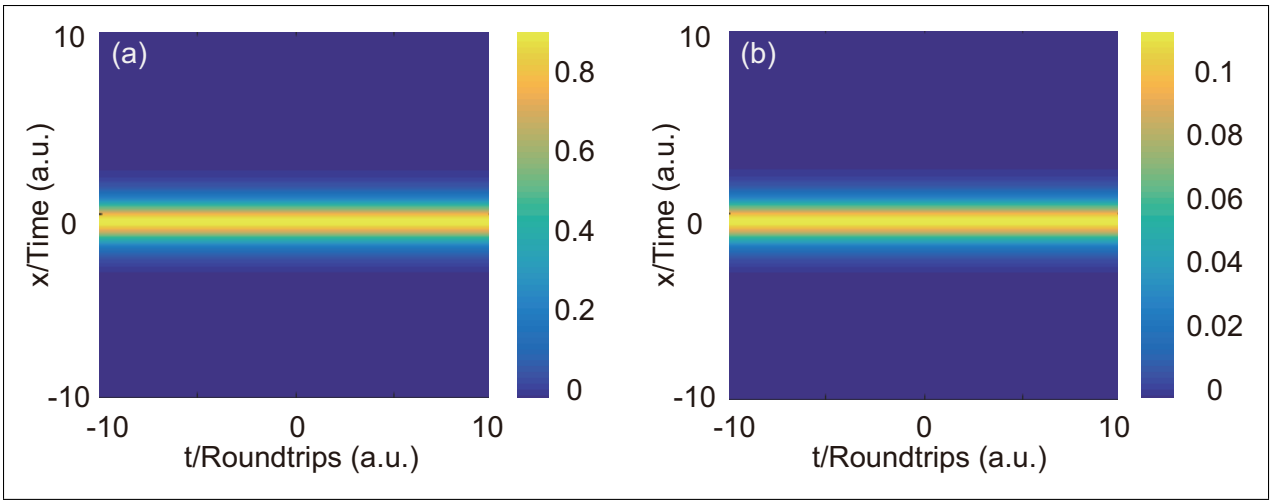

Figure 3: Due to the splitting of dual core fiber, the two sets of pulses correspond to the evolution diagram of non-degenerate bright soliton pulses of two-component BEC (a_1=a_2=0, b_1=b_2=1, β_1=2, β_2=0, γ_2=-γ_1=0.7). (a-b) Pulses evolution corresponding to the higher and lower energy in Fig. 2(e).

solutions must be corrected in the first step Ω_1 make constraints so that $\Omega_{21} = 0$ (or $\Omega_{31} = 0$), which means that the corresponding coefficient $\beta_1 = 0$ (or $\gamma_1 = 0$), and the spectral parameter is $\omega_1 = a_1 + ib_1$ Then, the nondegenerate bright soliton solution can be calculated by twice DT[25,26] calculation.

Fig. 3 shows the two sets of pulses correspond to the non-degenerate bright soliton pulses evolution diagram of two- components BEC. The 'x' presents the lateral evolution of a component pulse, which is similar to the 'Time' coordinate of DFT evolution. The other 't' coordinate is similar to the 'round trip' coordinate of DFT evolution. These all represent evolution states of the pulse form with the variation of time or the number of round trips in the cavity. Akin to the DFT evolution result of the pulse in Fig. 2(e), the two-component pulses are in a single envelope. Meanwhile, it keeps the result that one pulse intensity is large than the other pulse. This result is attributed to the fact that the energy of single-mode fiber is not evenly distributed through double core fiber.

When continuously increasing the pump power to 550 mW, the spectrum is shown in Fig. 4 (a). It can be seen the central wavelength and 3dB bandwidth are similar with the results under 490mW pumped power. However, the temporal pulse trains changes from a

Preprints (www.preprints.org) | NOT PEER-REVIEWED | Posted: 24 October 2022 doi:10.20944/preprints202210.0243.v2

single repetitive pulse sequence to four sets of periodically evolving time pulse sequences, as shown in Fig. 4(b). The phenomenon is due that the nonlinear effect in the cavity becomes stronger and the activities between solitons are intensified frequently, resulting in more coupling and collision opportunities between pulses, which will make the GVLVS change from a stable pulse complex to PRVS. Different from the ordinary two groups of PRVS effects ,[27,28] Fig. 4(b) shows the envelope evolution of the four components, and the

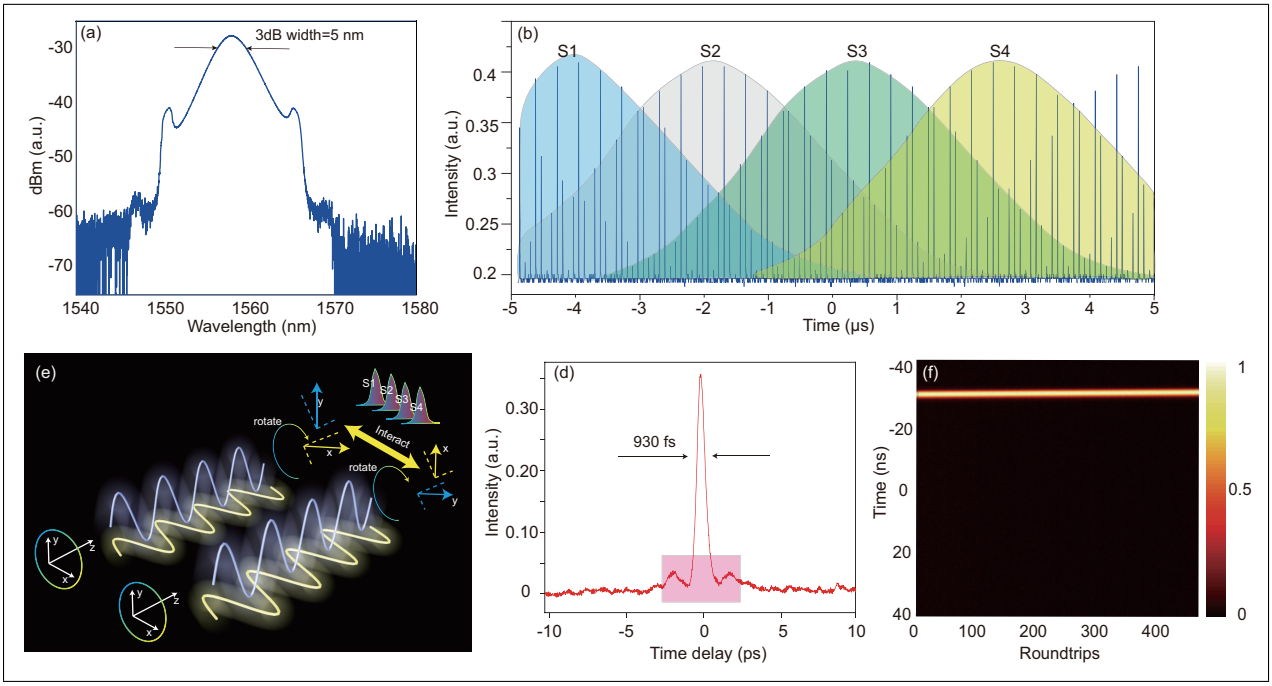

Figure 4: (a) Optical spectrum; (b) temporal pulse trains based on the oscilloscope; (c) schematic diagram of four pulse formation; (d) the autocorrelation evolution trace. (e) Results of DFT.

phase delay of each component exactly corresponding to $\pi/2$. It is calculated according to temporal evolution of oscilloscope. This phenomenon is easily explained from Fig. 4(c). Due to the weak coupling effect of SDCF, two groups of light run in the same cavity. However, the x-polarized and y-polarized components of each group will interact after entering the single-mode fiber. It should be noted that the corresponding x-polarized light and y-polarized light will rotate the polarization plane because of the nonlinear effect, which will cause the polarization component of x-polarized light in one core to interact with x-polarized light

Preprints (www.preprints.org) | NOT PEER-REVIEWED | Posted: 24 October 2022 doi:10.20944/preprints202210.0243.v2

and y-polarized light in another core at the same time and vice versa. Finally, the two polarization components of the two cores interfere with each other and then lock the mode, so there are four pulses. Since the two cores act in pairs and the x-polarized light and y-polarized light of each core are relatively bound, the final four pulses should be formed as a whole, which is different from the separate pulses shown in Fig. 2. In order to prove this phenomenon, the autocorrelation tracking and DFT evolution of pulses are studied, as shown in the Fig. 4(d) and Fig. 4(e). It can be seen from the autocorrelation spectrum that the pulse width is 930fs. Note of, there are two side lobes at the bottom of the pulse, which indicates that the pulse has the generation of bound state. However, the pulse side lobe base is not high, which proves that the pulse effect of forming bound state is weak, and strong nonlinearity is accumulated in the fiber cavity. Besides, it can be seen from Fig. 4(e) that DFT has only one soliton evolution track, which is different from two-core form the shape of solitons separately in Fig. 2. It also proves the formation of PRVS is related to the interaction of two cores, rather than the formation of independent cores.

When the pump power continues to increase to 570mw, the multi-pulse state begins to appear with the nonlinearity gradually accumulating in the cavity. At this time, there are multiple solitons in the cavity, The energy of these solitons is unequal, and the interval is different. The pulses also exist the phenomenon of self-walking away. These characteristics indicate the cavity is in a very unstable state. By fine adjusting the polarization controller in the cavity, the energy distribution of vector solitons is uniform, and the interaction force begins to expand gradually to the entire pulse duration. Then, all solitons gradually show the state of equal spacing. The overall shape of the soliton spectrum in Fig. 5(a) shows obvious spectral modulation characteristics, which is a typical spectrum of double soliton bound states. The spectral center wavelength of the bound state soliton is 1563 nm and the modulation period is 2.6 nm. This spectral modulation is essentially the result of stable interference between vector solitons constituting bound states. From the pulse sequence diagram in Fig. 5(b), it can be seen that after fine-tuning PC, the vector soliton is split

Preprints (www.preprints.org) | NOT PEER-REVIEWED | Posted: 24 October 2022 doi:10.20944/preprints202210.0243.v2

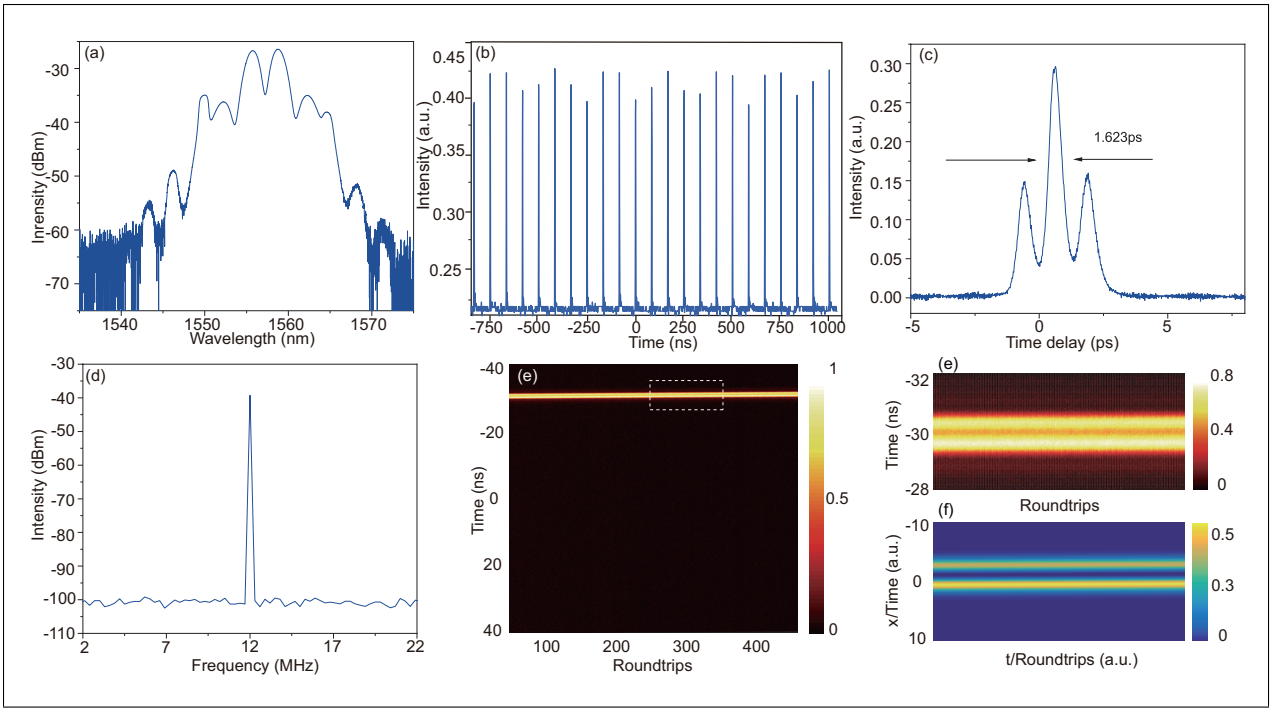

Figure 5: (a) Optical spectrum; (b) temporal pulse trains based on the oscilloscope; (c) the autocorrelation evolution trace; (d) RF spectrum; (e) Results of DFT; (f) Local enlargement of pulse evolution; (g) the two sets of pulses correspond to the evolution diagram of non-degenerate bright soliton pulses of two components of BEC (a_1=a_2=0, b_1=1.1, b_2=1.2, β_1=β_2=1, γ_2=γ_1=0.8)

into multiple pulses, and three spikes appear on the autocorrelation curve shown in Fig. 5(c), which proves again that the bound state obtained at this time is a double soliton bound state. The pulse width is assumed to be hyperbolic secant with a pulse width of 1.623 ps. The distance between the main peak and the side peak on the autocorrelator curve is 3.8ps, which is the distance between the two solitons constituting the bound state. If the spectral modulation period is converted into frequency, the product of the spectral modulation period and the soliton spacing is 1. At this time, the soliton spacing of 3.8ps matches the spectral modulation period of 2.6nm. It can be seen soliton spacing is less than 5 times the pulse width, which indicates that the tightly bound state is observed in the experiment. The formation of this tightly bound state comes from the direct interaction between adjacent solitons. The corresponding RF spectrum is shown in Fig. 5(d), showing a repetition frequency of 12MHz and a signal-to-noise ratio (SNR) of 60dB. It can be seen that

Preprints (www.preprints.org) | NOT PEER-REVIEWED | Posted: 24 October 2022 doi:10.20944/preprints202210.0243.v2

bound state solitons have strong anti-interference ability. For exploring the formation process of bound state pulses involved in SDCF, the DFT evolution of pulses was characterized in Fig. 5(e). Obviously, there is only one path for the evolution of the pulse complex. It is proved that the formation of two solitons is not the mode-locked pulse reaction formed in two cores respectively, but the solitons formed by the interference of their respective polarization components between the two cores. The corresponding double solitons interference evolution path is consistent with the pulse complex formed by the interaction of double solitons in a traditional single core laser cavity. In addition, the bound state of stable interference proves that there is a stable phase difference between solitons. Then, we also utilizing the Eq. (1) to analyze the evolution of non-degenerate bright soliton pulses of two-component of BEC in Fig. 5(e). At the different soliton phase, the evolution of non-degenerate bright soliton pulses is similar with the bound state soliton DFT in SDCF. It also shows that the soliton interaction based on SDCF can be well used to study the BEC of bright solitons based on two-component or multi-component. In this state, the PC is reasonably adjusted, and the pulse in the laser cavity is split to form multi-pulses with different peak amplitude. In the time domain, the main pulse with strong peak amplitude moves in one direction from right to left, while the secondary pulse with low peak amplitude moves in the opposite direction, which is similar to floating soliton. After the superposition of the secondary pulse and the main pulse, the intensity of the main pulse increases and the secondary pulse decreases. The specific situation is shown in the pulse sequence diagram of Fig. 6(a)-(b), the phenomenon of redistribution of primary and secondary pulse energy after overlapping may be due to the gain competition between pulses due to the quantum effect of soliton energy. The whole soliton dynamic evolution process in the cavity is similar to the soliton rain state. The reason is that the dispersive wave in the laser cavity is not effectively filtered, which will resulting in an increase of dispersive wave strength after passing through the gain fiber. In this way, the coexistence state of strong dispersive wave and soliton wave will appear in the cavity, and the complex interaction between them leads to the formation of

Preprints (www.preprints.org) | NOT PEER-REVIEWED | Posted: 24 October 2022 doi:10.20944/preprints202210.0243.v2

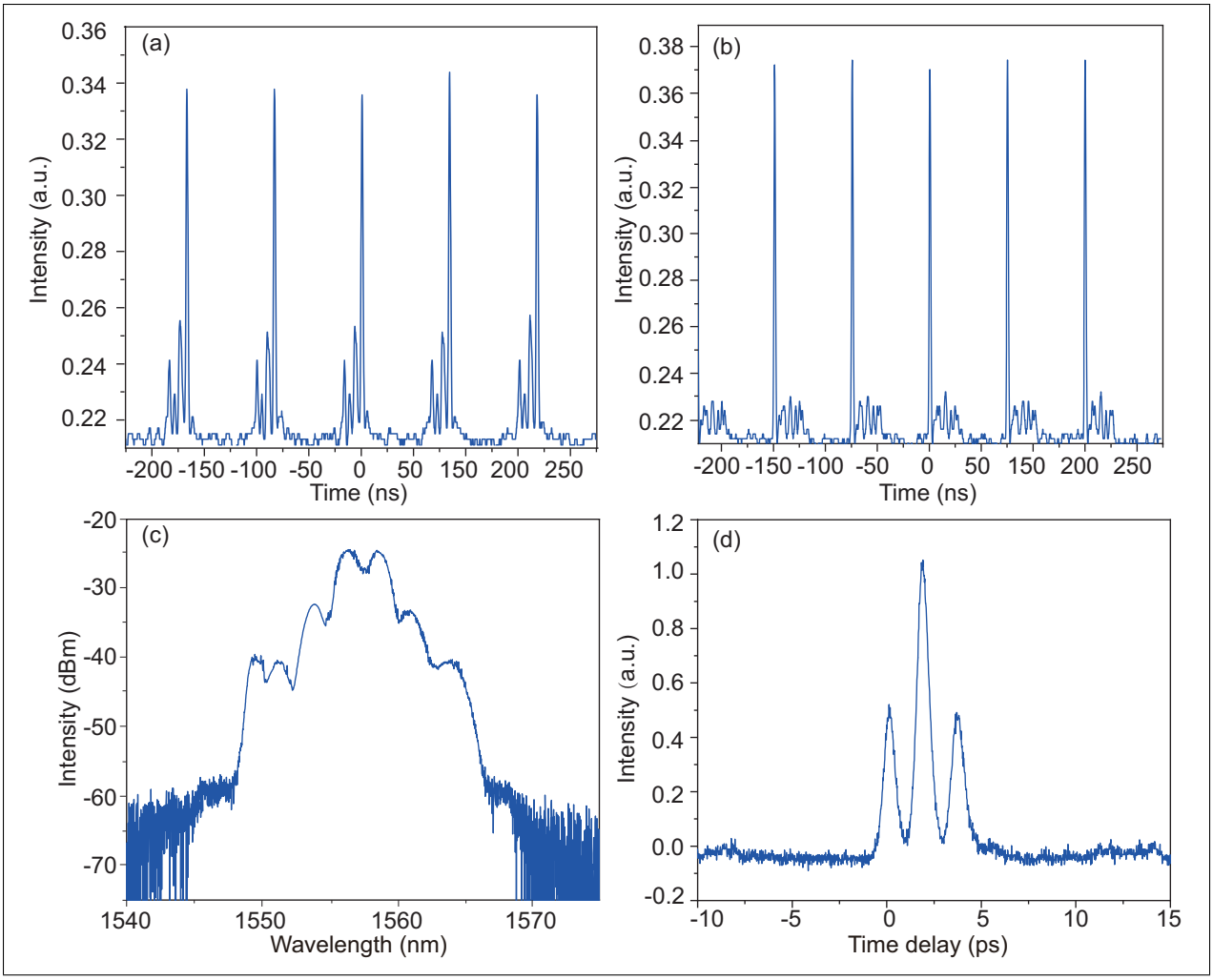

Figure 6: (a)-(b) temporal pulse trains based on the oscilloscope; (c) Optical spectrum; (d) the autocorrelation evolution trace.

soliton rain. As for the directional motion of soliton rain, it is that the complex interaction between dispersive waves and soliton waves lead to resonant energy exchange, which will produce the energy flow direction of soliton rain. Fig. 6 (c) shows the spectrum of soliton rain, which indicates the obvious quasi periodic modulation characteristics, which is similar to the spectral characteristics of the interaction between different solitons in bound state solitons. It is not only the interaction between dispersive wave and solitons (with traditional Kelly sideband characteristics), but also the interaction between different quasi bound state solitons (with quasi periodic modulation characteristics) induced by dispersive wave. These can also demonstrate that there is a complex interaction between dispersive wave and soliton

Preprints (www.preprints.org) | NOT PEER-REVIEWED | Posted: 24 October 2022 doi:10.20944/preprints202210.0243.v2

wave. What's more, this interaction is also one of the main factors leading to soliton rain. The bound state shape of soliton splitting appears on the autocorrelation curve shown in Fig. 6(d), which shows that the interaction between soliton molecules leads to the generation of soliton rain state, and its pulse width is 900fs. Furthermore, the soliton rain state based on

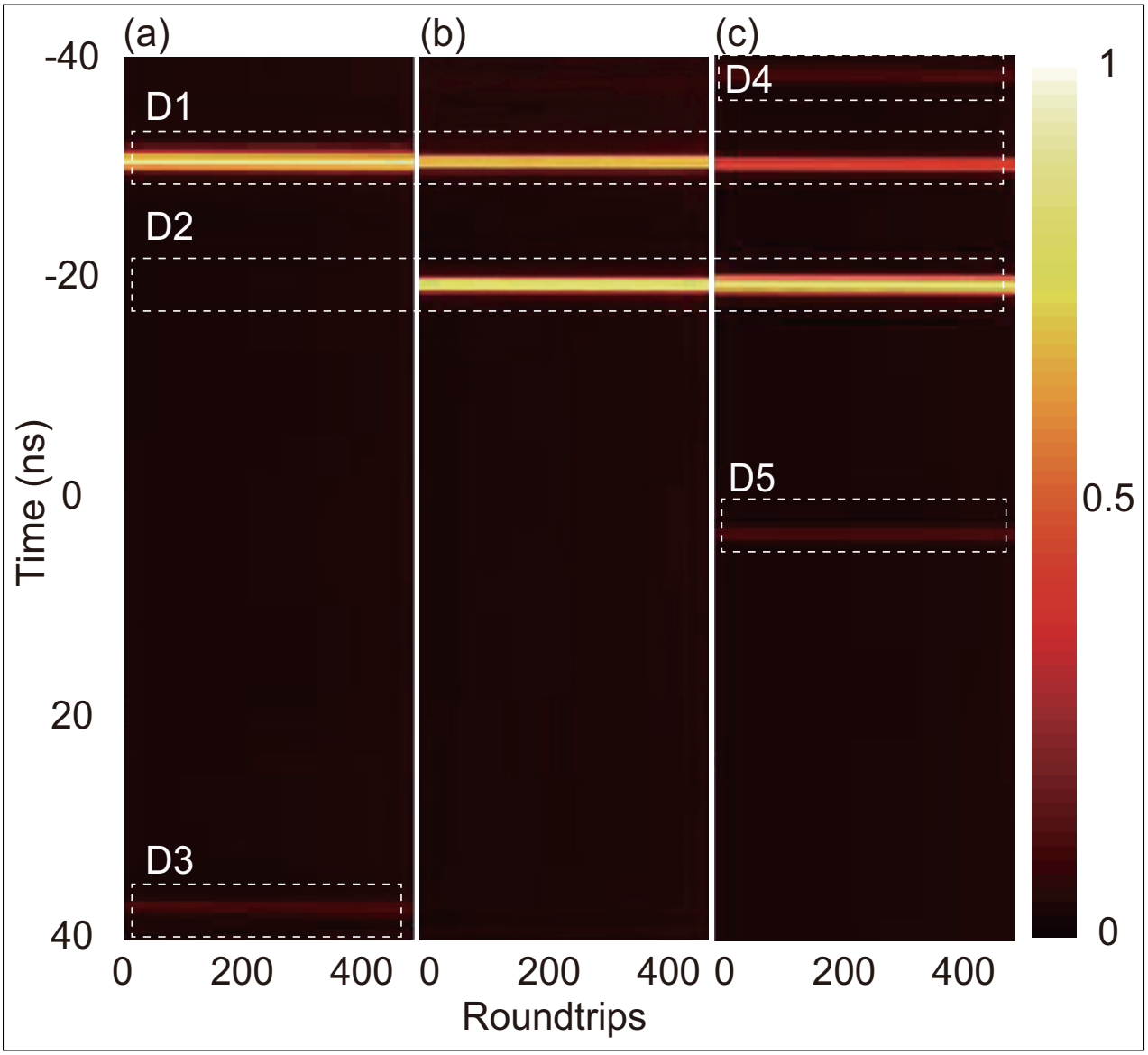

Figure 7: (a)-(c) Results of DFT under different temporal pulse trains.

SDCF is observed by DFT technology as shown in Fig. 7. It can be seen that the generation and annihilation of five pulses D1-D5 appear in the continuous evolution of soliton rain pulses. It is worth noting that this state is produced in the bound state. Therefore, the bound state

 doi:10.20944/preprints202210.0243.v2

pulse in D1 region is consistent with the evolution form of DFT pulse in Fig. 7(a). In addition, from the evolution of D2 region in Fig. 7(b) and Fig. 7(c), it can be seen that the generation process of soliton rain also has the evolution of four PVRS corresponding to Fig. 4. However, this state is not stable due to the influence of the generation and annihilation of other solitons in the soliton rain. It arises from D1 in Fig. 7(a) and then floats and disappears in the time domain. Besides, other solitons, such as those in D3, D4 and D5 regions, are constantly generated and disappear from the bound state in D1 region in the laser cavity because they are in an unstable locking state. It can be seen from Figs. 7 (a) - (c) that as the number of solitons increases, the energy of the bound state, i.e., D1 region, will decrease, but the total energy remains unchanged. The abundant pulse interference in the cavity is also due to the generation of space division multiplexing pulses caused by weakly coupled dual cores of SDCF.

Conclusions

In summary, we characterize the vectorial solitons nature in SDCF assisted ultrafast fiber lasers. Because of the separate of dual cores in SDCF, there are two sets of mode-locked pulses in a single laser cavity. On the basis of conventional group velocity locked pulses, due to the non-degeneracy of two sets of mode-locked optical paths, starting from the action mechanism of non-degenerate bright solitons in BEC effect, the formation of two component non-degenerate bright solitons is studied equivalently. The pulse evolutions are in good agreement with the experimental DFT results. It is proved that the multi-core fiber mode-locked laser provides an equivalent platform for the study of multicomponent solitons in BEC condensates. Beyond the most fundamental group velocity locked vector soliton, the four component PRVS, which is different from the traditional polarization rotation vector soliton, is generated in the cavity because two sets of mode-locked optical paths in the dual core coexist in one cavity. The generation of soliton bound states is realized by further increasing

 doi:10.20944/preprints202210.0243.v2

the pump power and nonlinearity. It is found that there is only a one path for the evolution of the pulse complex, which proved that the solitons in the two cavities form a stable pulse binding through the mutual interference between the fiber core. On this basis, the evolution of multi pulse soliton rain in the above bound state can be formed by adding a certain bias phase to the pulse in the cavity. Then, the abundant pulse interference in the cavity is due to the generation of space division multiplexing pulses caused by weakly coupled dual cores of SDCF. All these findings can spread new perspectives into spatiotemporal vectorial solitons dynamics with more degrees of freedom and highlight the possible application for optical frequency comb, verification physical phenomena of BEC.

Acknowledgement

National Key Research and Development Program of China (Grant No. 2019YFB2204002), Key Project of Basic Research and Applied Basic Research in Ordinary Universities of Guangdong Province (2018KZDXM067), Department of Science and Technology of Guangdong Province (2020B1515120041).

References

(1) Fermann, M. E.; Hartl, I. Ultrafast fibre lasers. *Nature photonics* **2013**, *7*, 868–874.

(2) Jauregui, C.; Limpert, J.; Tünnermann, A. High-power fibre lasers. *Nature photonics* **2013**, *7*, 861–867.

(3) Cundiff, S. T.; Weiner, A. M. Optical arbitrary waveform generation. *Nature Photonics* **2010**, *4*, 760–766.

(4) Shang, X.; Guo, L.; Zhang, H.; Li, D.; Yue, Q. Titanium disulfide based saturable absorber for generating passively mode-locked and Q-switched ultra-fast fiber lasers. *Nanomaterials* **2020**, *10*, 1922.

(5) Richardson, D. J.; Laming, R. I.; Payne, D. N.; Matsas, V.; Phillips, M. W. Self-starting, passively mode-locked erbium fibre ring laser based on the amplifying Sagnac switch. *Electronics Letters* **1991**, *27*, 542–544.

(6) Ilday, F.; Wise, F.; Sosnowski, T. High-energy femtosecond stretched-pulse fiber laser with a nonlinear optical loop mirror. *Optics letters* **2002**, *27*, 1531–1533.

(7) Luo, Y.; Xia, R.; Shum, P. P.; Ni, W.; Liu, Y.; Lam, H. Q.; Sun, Q.; Tang, X.; Zhao, L. Real-time dynamics of soliton triplets in fiber lasers. *Photonics Research* **2020**, *8*, 884–891.

(8) Schön, S.; Haiml, M.; Keller, U. Ultrabroadband AIGaAs/CaF 2 semiconductor saturable absorber mirrors. *Applied Physics Letters* **2000**, *77*, 782–784.

(9) Liu, X.; Han, D.; Sun, Z.; Zeng, C.; Lu, H.; Mao, D.; Cui, Y.; Wang, F. Versatile multi-wavelength ultrafast fiber laser mode-locked by carbon nanotubes. *Scientific reports* **2013**, *3*, 1–6.

(10) Zhang, H.; Lu, S.; Zheng, J.-l.; Du, J.; Wen, S.; Tang, D.; Loh, K. Molybdenum disulfide (MoS 2) as a broadband saturable absorber for ultra-fast photonics. *Optics express* **2014**, *22*, 7249–7260.

(11) Liu, K.; Xiao, X.; Ding, Y.; Peng, H.; Lv, D.; Yang, C. Buildup dynamics of multiple solitons in spatiotemporal mode-locked fiber lasers. *Photonics Research* **2021**, *9*, 1898–1906.

(12) Liang, H.; Zhao, X.; Liu, B.; Yu, J.; Liu, Y.; He, R.; He, J.; Li, H.; Wang, Z. Real-time dynamics of soliton collision in a bound-state soliton fiber laser. *Nanophotonics* **2020**, *9*, 1921–1929.

(13) Lyu, Y.; Shi, H.; Wei, C.; Li, H.; Li, J.; Liu, Y. Harmonic dissipative soliton reso-

nance pulses in a fiber ring laser at different values of anomalous dispersion. *Photonics Research* **2017**, *5*, 612–616.

(14) Fang, J.-J.; Mou, D.-S.; Wang, Y.-Y.; Zhang, H.-C.; Dai, C.-Q.; Chen, Y.-X. Soliton dynamics based on exact solutions of conformable fractional discrete complex cubic Ginzburg–Landau equation. *Results in Physics* **2021**, *20*, 103710.

(15) Luo, W.; Liu, X.; Li, X.; Lv, S.; Xu, W.; Wang, L.; Shi, Z.; Zhang, C. SnSe2 realizes soliton rain and harmonic soliton molecules in erbium-doped fiber lasers. *Nanotechnology* **2021**, *32*, 165203.

(16) Kbashi, H. J.; Sergeyev, S. V.; Al Araimi, M.; Tarasov, N.; Rozhin, A. Vector soliton rain. *Laser Physics Letters* **2019**, *16*, 035103.

(17) Xu, S.; Turnali, A.; Sander, M. Y. Group-velocity-locked vector solitons and dissipative solitons in a single fiber laser with net-anomalous dispersion. *Scientific Reports* **2022**, *12*, 1–8.

(18) Chen, G.; Li, W.; Wang, G.; Zhang, W.; Zeng, C.; Zhao, W. Generation of coexisting high-energy pulses in a mode-locked all-fiber laser with a nonlinear multimodal interference technique. *Photonics Research* **2019**, *7*, 187–192.

(19) Boggio, J.; Bodenmüller, D.; Ahmed, S.; Wabnitz, S.; Modotto, D.; Hansson, T. Efficient Kerr soliton comb generation in micro-resonator with interferometric back-coupling. *Nature communications* **2022**, *13*, 1–11.

(20) Wright, L. G.; Christodoulides, D. N.; Wise, F. W. Spatiotemporal mode-locking in multimode fiber lasers. *Science* **2017**, *358*, 94–97.

(21) Runge, A. F.; Broderick, N. G.; Erkintalo, M. Observation of soliton explosions in a passively mode-locked fiber laser. *Optica* **2015**, *2*, 36–39.

 doi:10.20944/preprints202210.0243.v2

(22) Hui, Z.; Xu, W.; Li, X.; Guo, P.; Zhang, Y.; Liu, J. Cu 2 S nanosheets for ultrashort pulse generation in the near-infrared region. *Nanoscale* **2019**, *11*, 6045–6051.

(23) Zhao, L.-C.; Liu, J. Localized nonlinear waves in a two-mode nonlinear fiber. *JOSA B* **2012**, *29*, 3119–3127.

(24) Kevrekidis, P.; Frantzeskakis, D. Solitons in coupled nonlinear Schrödinger models: a survey of recent developments. *Reviews in Physics* **2016**, *1*, 140–153.

(25) Doktorov, E. V.; Leble, S. B. *A dressing method in mathematical physics*; Springer Science & Business Media, 2007; Vol. 28.

(26) Ling, L.; Zhao, L.-C.; Guo, B. Darboux transformation and multi-dark soliton for N-component nonlinear Schrödinger equations. *Nonlinearity* **2015**, *28*, 3243.

(27) Liu, M.; Luo, A.-P.; Luo, Z.-C.; Xu, W.-C. Dynamic trapping of a polarization rotation vector soliton in a fiber laser. *Optics Letters* **2017**, *42*, 330–333.

(28) Akosman, A. E.; Zeng, J.; Samolis, P. D.; Sander, M. Y. Polarization rotation dynamics in harmonically mode-locked vector soliton fiber lasers. *IEEE Journal of Selected Topics in Quantum Electronics* **2017**, *24*, 1–7.

Preprints (www.preprints.org) | NOT PEER-REVIEWED | Posted: 24 October 2022 doi:10.20944/preprints202210.0243.v2

TOC Graphic